

Robust, Probabilistic, Constraint-Based Localization for Wireless Sensor Networks

Rong Peng and Mihail L. Sichitiu

Department of Electrical and Computer Engineering

North Carolina State University

Raleigh, NC 27695

email: {rpeng,mlsichit}@ncsu.edu

Abstract—Localization is a fundamental service for many applications in wireless sensor networks. In this paper we propose a probabilistic, constraint-based approach robust to range measurement inaccuracies. The proposed approach proceeds in three phases: the first phase involves modeling the uncertainties of range measurements; in the second phase, a set of probabilistic constraints are computed and combined to produce initial position estimates; in the final phase, negative constraints are used to refine the initial estimates. We evaluated the proposed approach through simulations based on real-world measurements; the results are compared with two other localization schemes and the Cramer-Rao lower bound. The results show that, for inaccurate range measurements, the proposed probabilistic approach performs the best and close to the optimal bound.

I. INTRODUCTION

Recent advances in wireless communications, low power sensors and microcontrollers enabled a new wide area monitoring paradigm commonly known as wireless sensor networking [1]–[3]. Wireless sensor networks (WSNs) allow for inexpensive, high quality monitoring of large geographical areas. WSNs are usually implemented as a (potentially large) number of wireless sensor nodes that communicate over multiple hops to one or more base stations.

Many WSN applications either require, or benefit from a localization service that provides the position of each sensor node. Simply knowing *where* an event occurs is a requirement for many of these applications. Tracking, which is a classical WSN application, requires good localization (and synchronization).

Perhaps the simplest method of providing localization is to equip every sensor node with a GPS receiver (assuming that the sensor nodes are deployed outdoors with a clear view of the sky). However, a GPS receiver is expensive in terms of money (target prices for sensor nodes are around \$1), size and energy. Another alternative is hand-placing each sensor and manually recording its position. This is a tedious and error prone approach unsuitable for large sensor networks and many of the proposed WSN applications.

The most common alternative for localizing the nodes involves using a limited number of nodes (perhaps the base stations) equipped with GPS receivers (called *beacon* or *anchor nodes*) to localize all the other nodes (commonly called

unknown nodes).

Two large classes of localization systems have been proposed:

- **Range free** (or proximity based) approaches infer constraints on the proximity to beacon nodes. These approaches, although attractively simple (they do not require any additional hardware and most require only simple operations), have inherently limited precision.
- **Range based** approaches rely on range measurements to compute the position of the unknown nodes. Most existing approaches assume exact (or almost exact) range measurements and are shown to perform very well when this assumption is satisfied.

However, accurate range measurements currently require specialized (often expensive) hardware. In contrast, received signal strength (RSS) information is always available in practically all transceivers suitable for wireless networks. The main drawback of RSS-based measurements is their (relatively large compared with other methods) inaccuracy.

In this paper we extend our previous research on WSN localization [4], [5]. We propose a localization method suitable for inaccurate range measurements (such as those from RSS measurements); the method performs significantly better than proximity-based approaches, while allowing for inexpensive implementations. We show that, for inaccurate range measurements, the proposed approach performs better than existing approaches and very close to the optimum (obtained from the Cramer-Rao bound).

II. RELATED WORK

There has been a significant research activity in the area of localization. In this section we provide a brief literature review.

Range-based schemes:

RADAR [6] is a range-based indoor localization system that measures RSS at all positions in the entire building and records the RSS into a database during the calibration phase. In the localization phase, the location and the orientation of a user are determined by finding the best match of a set of RSS measurements in the database. The Cricket indoor localization support system [7] utilizes a combination of RF and ultrasound measurements to provide location information to users. In

APS [8], [9] a range-free (the DV-hop) and two range-based (the DV-distance and Euclidean) methods are used to obtain distance estimates between unknown nodes and beacons; the distances are then used to locate the unknown nodes by trilateration. Multilateration [10], [11] (an iterative least square scheme) can also be used to determine the positions of the unknown nodes given (potentially incompatible) distance measurements to several beacons. In [12], network connectivity is used for the initial position estimates and triangulation is used to refine the estimation. An approach for finding the *relative* position of the nodes in the absence of GPS assistance is presented in [13]. Another relative localization method is proposed in [14]: robust quadrilaterals are used to reduce the effect of flip ambiguities caused by inaccurate distance measurements. A scheme tolerant to anisotropic network scenarios [15] uses multidimensional scaling (MDS) to calculate the relative positions of the unknown nodes; the absolute positions are determined using coordinate alignment techniques. In [4], [5] we demonstrated the feasibility of RSS-based probabilistic localization on a small outdoor testbed with iPAQs and 802.11 wireless cards. Directionality-based schemes using the angle of arrival (AOA) between neighbor nodes are proposed in [16], [17].

Range-free schemes:

The active badge system [18] is an indoor range-free system using infrared (IR) for signaling between the sensors and the badges worn by personnel. The location of a badge can be found given the positions of the sensors. In [19], a node localizes itself at the centroid of the overlapped transmission coverage regions of the beacon nodes. A set of connectivity constraints are built in [20], which are used to discover the location by convex optimization. With the assistance of a moving target, a deterministic constraint-based localization approach is proposed in [21] using bounding rectangles and negative information. In [22], an area-based range-free localization scheme is presented; the position uncertainty of an unknown is reduced by using the triangles formed by all the beacons that can be heard by that unknown.

The proposed localization approach belongs to the class of range-based schemes. The main difference from existing localization schemes is that the proposed approach assumes inaccurate range measurements. The inaccuracies are characterized by modeling the range measurements as a set of probability density functions. These functions are used to compute probabilistic constraints that reduce the uncertainties of the nodes' positions. Probabilistic negative constraints are introduced in this paper to further improve the estimation accuracy and precision. To the best of our knowledge, probabilistic negative information have not been proposed in literature. The proposed approach is developed for two dimensional spaces, but can be easily extended to three-dimensions.

III. PROPOSED APPROACH

The proposed approach is fully distributed. Every unknown node estimates its own position using a probability density function (pdf) $f_{X,Y}(x,y)$ of the two-dimensional coordinate

variable (X,Y) . Therefore, the probability of an unknown being placed at the coordinate (x_ζ, y_ζ) is:

$$Prob(x_\zeta, y_\zeta) \approx \int_{y_\zeta - \Delta y}^{y_\zeta + \Delta y} \int_{x_\zeta - \Delta x}^{x_\zeta + \Delta x} f_{X,Y}(x,y) dx dy, \quad (1)$$

where $x_{min} \leq x \leq x_{max}$ and $y_{min} \leq y \leq y_{max}$. The probability $Prob(x_\zeta, y_\zeta) = Prob(X = x_\zeta, Y = y_\zeta)$, the constants $x_{min}, x_{max}, y_{min}$ and y_{max} are the bounding coordinates of the network, and both Δx and Δy are arbitrarily small values. The higher the probability $Prob(x_\zeta, y_\zeta)$, the more likely that the unknown node is placed at (x_ζ, y_ζ) . We decompose the localization in three distinct phases: calibration, positive constraint localization and negative constraint localization.

A. Phase I. Calibration and Statistical Processing

The wireless channel is notorious for its randomness and unpredictability [23]. We assume an outdoor environment without major obstructions. During the calibration phase we measure the RSS at different distances between a transmitter and a receiver pair. Let P and D denote the random variables of RSS (in dB) and distance (in meters), respectively. The mean of the RSS measurements $\bar{P}(d)$ and the standard deviation $\sigma_P(d)$ at each distance $D = d$ can be calculated from the calibration measurements; $\bar{P}(d)$ and $\sigma_P(d)$ can be used to generate a mapping from any RSS to a pdf of the distance random variable D .

Both in theory [23] and in our experiments, $\sigma_P(d)$ does not vary significantly with the distance. Let $\sigma_P(d) \approx \sigma_P, \forall d$. The RSS P at any fixed distance d is log-normally distributed [23]:

$$P[dB] = \bar{P}(d)[dB] + X_{\sigma_P}[dB], \quad (2)$$

$$\bar{P}(d)[dB] = P_0[dB] - 10n \lg\left(\frac{d}{d_0}\right), \quad (3)$$

where n is the path loss exponent, the random variable X_{σ_P} is caused by shadowing effects and have a Gaussian distribution with zero mean and standard deviation of σ_P . Both n and σ_P are dependent on the physical environment and can be determined from the calibration data; d_0 is the close-in reference distance and P_0 is the RSS at d_0 . Without loss of generality [23], we assume $d_0 = 1m$. Clearly, if no randomness exists in (2), namely, when $X_{\sigma_P} = 0$, an RSS of $P = p$ can be uniquely mapped to a distance \bar{d} with a probability of 1,

$$p \rightarrow Prob\{\bar{d} = 10^{\frac{P_0 - p}{10n}}\} = 1. \quad (4)$$

However, in reality, shadowing effects always exist. Based on the log-normal model (2), given a fixed RSS p , the distance D is log-normally distributed. Thereby, each RSS can be mapped uniquely to a pdf of D .

$$p \rightarrow \lg D \sim N(\mu_D(p), \sigma_D(p)), \quad (5)$$

$$\mu_D(p) = \lg \bar{d} + \sigma_D^2 \ln 10, \quad (6)$$

$$\sigma_D(p) = \sigma_D = \frac{\sigma_P}{10n}, \quad (7)$$

where \bar{d} is the same as shown in (4) and $\sigma_D(p)$ is constant.

Fig. 1 shows the statistic results of the calibrated data in one of our outdoor experiments [4]. In this experiment, Compaq 3870 iPAQs with Lucent Orinoco cards are used as sensor nodes. Received Signal Strength Indicator (RSSI) data is measured every 2.5m up to 50m. RSSI is an arbitrary integer value corresponding to the power strength of the received packets measured by the wireless card. The mean and three times the standard deviation of the calibrated RSSI at each distance are shown in Fig. 1. A log-normal shadowing model curve with $n = 2.94$ is also plotted to fit the calibration data. The exponent n is computed using logarithmic least square fitting. When the difference between the calibrated data and its fitting is small, parameters n and σ_P can be estimated and utilized to generate the mapping as in (5) - (7).

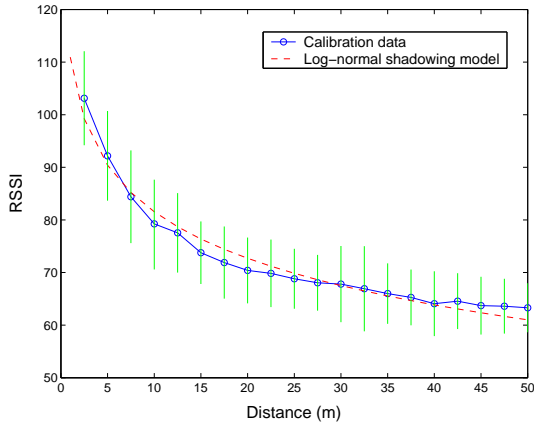


Fig. 1. Statistical mean and three times the standard deviation of the calibrated data together with a log-normal fit.

For environments with significant obstructions and severe multipath fading, the difference between the RSS mean $\bar{P}(d)$ (obtained from calibration measurements) at each distance and its log-normal fitting cannot be neglected; in these environments $\sigma_P(d)$ varies significantly with the distance as well. Given a fixed RSS $P = p$, using $\bar{P}(d)$ and $\sigma_P(d)$, the conditional pdf of D can be approximated as:

$$f_D(d|p) = \frac{\xi(d|p)}{\int_0^\infty \xi(d|p) dd}, \quad (8)$$

$$\xi(d|p) = \frac{1}{\sqrt{2\pi}\sigma_P(d)} e^{-\frac{(p-\bar{P}(d))^2}{2\sigma_P^2(d)}}. \quad (9)$$

From our outdoor calibration data, we found that, given an RSS measurement, the pdf of D can be mapped log-normally in the same format as (5) but with the mean $\mu_D(p) = E(\lg d|p)$ and the standard deviation $\sigma_D(p) = \sqrt{\text{Var}(\lg d|p)}$ of the variable D 's logarithm. In contrast to (6) and (7), both the mean and the standard deviation are functions of RSS and obtained statistically.

Fig. 2 shows the mapping from RSSI=83 to a log-normal distribution of the distance. We used the calibration measurements shown in Fig. 1. A log-normal mapping curve with

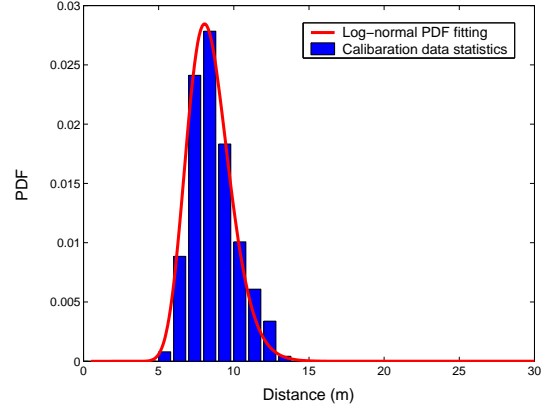


Fig. 2. Log-normal distribution of distances for packets with RSSI=83.

mean $\mu_D(\text{RSSI} = 83)$ and standard deviation $\sigma_D(\text{RSSI} = 83)$ fitting the bars is also plotted. The mean and the standard deviation are computed as described above. Fig. 2 shows that the distance for RSSI=83 has indeed a log-normal distribution as predicted. During the localization phase, we use the fitting curve to impose constraints on the position estimations of unknown nodes.

B. Phase II. Localization with Positive Constraints

In this phase, given the log-normal mappings of the RSS measurements, each unknown estimates its position pdf. Initially, each unknown sets its initial estimation to an even distribution over the entire network area, $f_{X,Y}(x,y) = \frac{1}{A}$, where A is the total area of the network. Nodes with position information, including both beacons and unknowns with updated pdf estimations, send out beacon packets to their neighbors. Upon receiving a beacon packet, an unknown executes the following algorithm:

- it measures the RSS of the received beacon packet;
- it maps the RSS to a one dimensional pdf obtained in phase I and generate a pdf constraint $\Psi_{X_C, Y_C}(x,y)$, which is a function of the coordinate random variable (X_C, Y_C) ;
- it updates the old pdf estimation by intersecting it with the generated constraint;
- finally, the unknown with the updated pdf estimation will broadcast to all its neighbors.

There are two classes of beacon packets:

- beacon packets from a beacon, and
- beacon packets from an unknown.

If the beacon packet is from a beacon b placed at (x_b, y_b) , we assume the position of the beacon is accurate (although the scheme may take into account any inaccuracies of the beacon's position). An unknown j within b 's transmission range receiving the beacon packet with RSS $p_{b,j}$ dB maps $p_{b,j}$ to a pdf of the distance with mean $\mu_D(p_{b,j})$ and standard deviation $\sigma_D(p_{b,j})$ as shown in (5); both $\mu_D(p_{b,j})$ and $\sigma_D(p_{b,j})$ are calculated during the first phase. The unknown j then

calculates a pdf constraint as:

$$\Psi_{X_C, Y_C}(x, y | p_{b,j}) = \frac{\phi(x, y, x_b, y_b)}{\int_{y_{\min}}^{y_{\max}} \int_{x_{\min}}^{x_{\max}} \phi(x, y, x_b, y_b) dx dy}, \quad (10)$$

$$\phi(x, y, x_b, y_b) = \frac{1}{\sqrt{2\pi}\sigma_D^2(p_{b,j})d_{b,j}} e^{-\frac{(\lg d_{b,j} - \mu_D(p_{b,j}))^2}{2\sigma_D^2(p_{b,j})}}, \quad (11)$$

$$d_{b,j} = \sqrt{(x - x_b)^2 + (y - y_b)^2}. \quad (12)$$

If the beacon packet is from an unknown node i with pdf estimation $f_{X_i, Y_i}(x, y)$, the unknown j , receiving a beacon packet from i with RSS $p_{i,j}$ dB, estimates the pdf constraints as:

$$\Psi_{X_C, Y_C}(x, y | p_{i,j}) = \frac{\phi(x, y)}{\int_{y_{\min}}^{y_{\max}} \int_{x_{\min}}^{x_{\max}} \phi(x, y) dx dy}, \quad (13)$$

$$\phi(x, y) = \int_{y_{\min}}^{y_{\max}} \int_{x_{\min}}^{x_{\max}} \phi(x, y, x_i, y_i) f_{X_i, Y_i}(x_i, y_i) dx_i dy_i, \quad (14)$$

where $\phi(x, y, x_i, y_i)$ has the same form as in (11) (with x_b substituted by x_i).

Assume the original pdf estimation for unknown j is $f_{X_j, Y_j}^{old}(x, y)$; a new pdf estimation for unknown j can be calculated by intersecting the pdf constraint described above, either from a beacon or an unknown, with the original estimation, if vector random variables (X_j, Y_j) and (X_C, Y_C) are mutually independent.

$$f_{X_j, Y_j}(x, y) = \frac{f_{X_j, Y_j}^{old}(x, y) \Psi_{X_C, Y_C}(x, y | p)}{\int_{y_{\min}}^{y_{\max}} \int_{x_{\min}}^{x_{\max}} f_{X_j, Y_j}^{old}(x, y) \Psi_{X_C, Y_C}(x, y | p) dx dy}. \quad (15)$$

Example

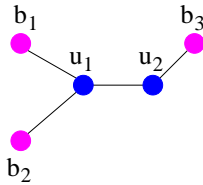


Fig. 3. Network topology with three beacons (b_1, b_2, b_3) and two unknowns (u_1, u_2).

Figure 3 depicts a network with three beacons (b_1, b_2, b_3) and two unknowns (u_1, u_2).

Assume the following sequence of events:

- Unknown u_1 uses the packets received from b_1 and b_2 to compute two constraints, which are intersected with each other to generate a new constraint. The new constraint is then intersected with the initial estimation (uniform distribution) to obtain a new pdf estimation as shown in Fig. 4(a).
- Unknown u_2 computes a pdf estimate of its position as shown in Fig. 4(b) using the beacon packet from b_3 .
- Both u_1 and u_2 send out beacon packets to their neighbors. When receiving the beacon packet from u_2 , u_1 calculates a pdf constraint as shown in Fig. 4(c).

- Node u_1 intersects the pdf constraint in Fig. 4(c) with its old pdf estimation in Fig. 4(a) to update its estimation. The results of the intersection is shown in Fig. 4(d).
- The same sequence is carried for u_2 (i.e., it computes the constraint and intersects it with the old pdf estimate). Using the beacon packet sent by u_1 , u_2 computes the pdf constraint shown in Fig. 4(e).
- Finally, u_2 intersects the constraint in Fig. 4(e) with its old pdf estimation in Fig. 4(b); the new pdf estimation of u_2 is shown in Fig. 4(f).

Intersecting the current position pdf estimation and the new constraint is only possible if the two vector random variables (X_j, Y_j) and (X_C, Y_C) are mutually independent. We will discuss how to combine the probabilities when dependencies occur (the realistic case) in Section IV-B.

The position of the unknown is determined at the place with the largest probability. The probability estimations for unknown u_1 and u_2 have the same shapes as their pdf estimations shown in Fig. 4(d) and Fig. 4(f), respectively. While the probability estimation for u_1 has only one peak which is at the true position of u_1 , however, the probability estimation for u_2 has two peaks, with the true position on lower peak. To improve the estimation accuracy and reduce the uncertainty, negative constraint are introduced in the next section.

C. Phase III. Localization with Negative Constraints

In this phase, we consider probabilistic negative constraints. In this enhancement, each unknown refines its probability estimation using negative constraints. The negative constraint is defined as a function $\rho(x, y)$ representing a constraint on an unknown when it cannot receive any packet from a given beacon. In other words, it is the information inferred from *not* hearing from a beacon.

Assume for the moment there is no shadowing effect and the minimum acceptable RSS is P_{min} (i.e., packets with RSS smaller than P_{min} will not be received); if beacon b is at (x_b, y_b) , an unknown j that is aware of the position of this beacon but unable to receive any packets from it can compute a negative constraint

$$\rho(x, y) = \rho(X_j = x, Y_j = y) \quad (16)$$

$$= \begin{cases} 0 & \text{if } d_{b,j} \leq d_{max} \\ 1 & \text{otherwise} \end{cases}, \quad (17)$$

where $d_{b,j}$ is calculated as shown in (12) and

$$d_{max} = 10^{\frac{P_0 - P_{min}}{10n}}. \quad (18)$$

Considering the shadowing effects (realistic case), the negative constraint can be calculated from calibration measurements. Recall that the RSS (in dB) at each distance is normally distributed as shown in (2). The negative constraint is then:

$$\rho(x, y) = \int_{-\infty}^{P_{min}} \frac{1}{\sqrt{2\pi}\sigma_P(d_{b,j})} e^{-\frac{(p - \bar{P}(d_{b,j}))^2}{2\sigma_P^2(d_{b,j})}} dp. \quad (19)$$

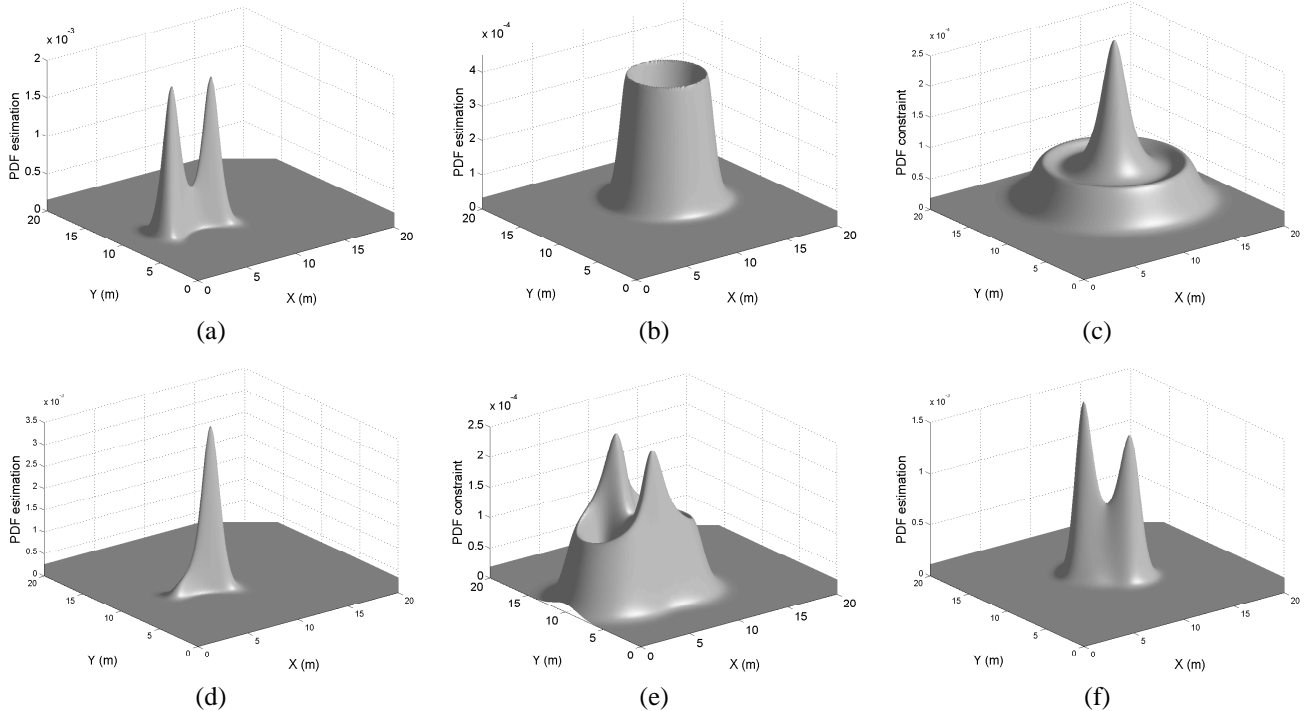


Fig. 4. Localization evolution for the network topology in Fig. 3 (a) pdf estimation of u_1 using beacon packets from b_1 and b_2 (b) pdf estimation of u_2 using beacon packet from b_3 (c) pdf constraint on u_1 calculated by using u_2 's beacon packet (d) Final position estimate of u_1 computed as the intersection of the old pdf estimation and the pdf constraint for u_1 (e) pdf constraint on u_2 calculated by using u_1 's beacon packet (f) Final position estimate of u_2 computed as the intersection of the old pdf estimation and the pdf constraint for u_2 .

Thus, the probability of unknown j is represented by the following probability:

$$\widetilde{Prob}(x,y) = \frac{Prob(x,y)\rho(x,y)}{\sum_{x_{min}}^{x_{max}} \sum_{y_{min}}^{y_{max}} Prob(x,y)\rho(x,y)}. \quad (20)$$

Example

Using the same network topology in Fig. 3, node u_2 can neither hear directly from b_1 nor b_2 . The intersection of the b_1 and b_2 's negative constraints is shown in Fig. 5(a). The final probability estimation for u_2 after intersecting the old one with the negative constraint is shown in Fig. 5(b). For u_2 's estimation, only one peak implying the true position left. In this case the negative constraint refinement clearly helps to reduce the estimation uncertainty and improve the estimation accuracy compared to Fig. 4(f). We will evaluate the usefulness of negative constraints for more general settings in Section V.

The final position estimation of the unknown j corresponds to the coordinates with the maximum probability.

$$(x^*, y^*) = \underset{x,y}{\operatorname{argmax}} \widetilde{Prob}(x,y). \quad (21)$$

IV. ALGORITHM DESIGN AND IMPLEMENTATION

In this section we will provide the details regarding the design of the algorithm that implements the ideas in Section III.

A. Packet and Log Format

The only nodes providing accurate position information are beacons, and all unknowns estimate their position based on

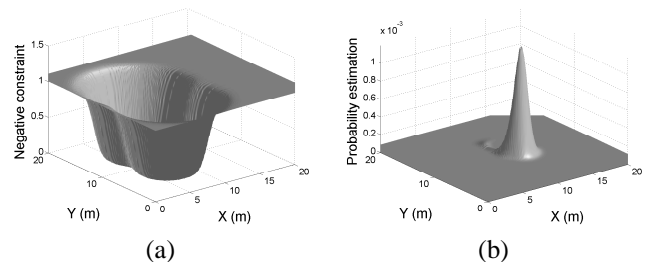


Fig. 5. Refinement using negative constraints (a) The intersection of b_1 's and b_2 's negative constraint (b) Final pdf estimation of u_2 after combining the negative constraints in (a) with the positive constraint estimate in Fig. 4(f).

this information. In the proposed algorithm each unknown stores a log as shown in Table I. All entries start with a beacon identifier (ID_{bi}) and the coordinates of the beacon (x_{bi}, y_{bi}). Each entry represents a transmission path from the beacon to the unknown node storing the log. ID_{ui} s are the IDs of the intermediate unknowns. A beacon can start multiple entries, as the first two entries shown in the table, since all the neighboring unknowns of the beacon relay its position information. Similarly, a single unknown can appear in multiple entries. Each unknown upon the receipt of a log entry from a neighbor node (beacon or unknown) appends its node ID to the log entry and records the RSS of the received packet. Beacon packets from an unknown contain one to several entries from that unknown's log. Packets from

beacon nodes follow the same format (having only the beacon information).

TABLE I
BEACON PACKET FORMAT.

Length	ID_b1	x_b1	y_b1	ID_u11	RSS11	ID_u12	RSS12	...
Length	ID_b1	x_b1	y_b1	ID_u21	RSS21	ID_u22	RSS22	...
Length	ID_b2	x_b2	y_b2	ID_u31	RSS31	ID_u32	RSS32	...
⋮	⋮	⋮	⋮	⋮	⋮	⋮	⋮	⋮

B. Dependency Elimination

The log processing involves eliminating dependencies among different log file entries. Recall that when vector random variables (X_j, Y_j) and (X_C, Y_C) are dependent, simple intersection between the pdf estimations and the constraints cannot be performed. We classify the dependencies in two categories:

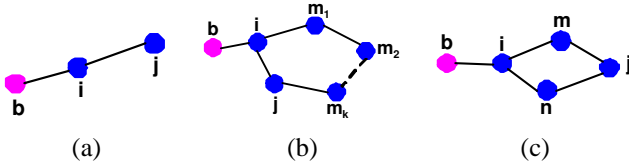


Fig. 6. Network topologies with dependencies (node b is a beacon, all the others are unknowns): (a) i to i dependency case 1 (b) i to i dependency case 2 (c) common i constraint dependency.

1) i to i dependency: Two typical cases of i to i dependency are shown in Fig. 6(a) and (b).

In Fig. 6(a), after computing its pdf estimation $f_{X_i, Y_i}(x, y)$ using packets from b , node i sends a beacon packet to unknown j . Unknown j , upon receiving the beacon packet, will recalculate its pdf estimate and broadcast the updates back to i . The new constraint calculated by i using the beacon packet sent by j is $\Psi_{X_C, Y_C}(x, y | p_{j,i})$, where $p_{j,i}$ is the RSS at i . It can be shown that (X_i, Y_i) is dependent on (X_C, Y_C) .

Fig. 6(b) shows another case with the same underlying dependency. Assume several unknowns (m_1, m_2, \dots, m_k) are on a path between unknowns i and j . Assume that node i propagates a beacon packet on the path $i \rightarrow m_1 \rightarrow m_2 \rightarrow \dots \rightarrow m_k \rightarrow j \rightarrow i$. Eventually, i will use the beacon packet from j to calculate constraint $\Psi_{X_C, Y_C}(x, y | p_{j,i})$. Just like in the case of in Fig. 6(a), (X_i, Y_i) and (X_C, Y_C) are dependent.

In summary, the i to i dependency occurs in a path (log entry) where one unknown occurs more than once.

2) *Common i constraint dependency*: Fig. 6(c) shows a common i constraint dependency scenario. Both m and n update their pdfs using beacon packets from unknown i and broadcast their updates to unknown j . Assume the beacon packet from m arrives first, j updates its pdf to $f_{X_j, Y_j}(x, y)$. Next j will use the beacon packet from n to calculate the pdf constraint $\Psi_{X_C, Y_C}(x, y | p_{n,j})$. Nevertheless, (X_m, Y_m) and (X_n, Y_n) are dependent, which results in the dependency between (X_j, Y_j) and (X_C, Y_C) .

In the common i constraint dependency scenario, two or more paths share one or more intermediate unknowns.

From the discussion above, if each node appears only once in a single row of the log file, no i to i dependency exists. Therefore, the first kind of dependency can be eliminated by deleting all the rows, in each of which an node has been recorded multiple times.

The common i dependency is eliminated by searching for all the rows that contain the same intermediate unknown with different descendent unknowns. Among all these rows, the longer paths (in terms of hops) are deleted first. Among all shorter paths, only one (randomly chosen) for every intermediate unknown is kept, others are discarded. This way the dependencies are eliminated.

After eliminating the dependency, the position pdf estimation can be computed by intersection. Each unknown uses the log file to calculate its probability estimation based on both positive and negative constraints.

Waiting Period

In order to reduce the traffic overhead, a waiting time can be inserted between the receiving of a beacon packet and the broadcasting of the update. Consider the scenario shown in Fig. 7 where both m and n are in the transmission range of beacon b and reachable by unknown i . Node i necessarily receives the beacon packets from m and n consecutively. In order for i to avoid sending two packets (one due to the packet received from m and another one for the packet from n), node i should wait for a time T before it broadcasts. Thus, it can *aggregate* the information from both node m and n before it sends the packet to node j . The time T should be chosen sufficiently large to allow all intermediate nodes to send their beacons.

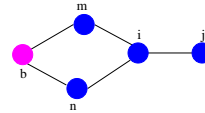


Fig. 7. Node i aggregates the beacon packets from unknowns m and n before broadcasting to unknown j .

The algorithm is repeated distributively at every unknown and, eventually, data from all beacon nodes will reach all the unknown nodes and the algorithm will stop. Alternatively, to reduce the number of messages, we can impose a lower threshold on the improvement that has to occur in the position of an unknown for that node to forward a beacon packet: information from beacons after it travels many hops is often too diluted (i.e., the constraints, do not constrain too much) to make any difference in the position of a node. Therefore, the compute procedure at an unknown will stop after a relatively stable estimation is achieved.

V. SIMULATION RESULTS

Meaningful evaluation of the proposed approach is not trivial. We showed the practical feasibility of other (single

hop and not considering negative information) probabilistic approaches [4], [5]. However, a practical experiment is limited with respect to the number of nodes and scenarios that can be considered.

On the other hand, current network simulators (e.g., ns-2, Qualnet, OPNET), do not consider realistic physical layer effects like the (unintended) directionality of the antennas and variability in the power of each radio.

Therefore, we decided to use a custom simulator, implemented in Matlab and using calibration data based on real world measurements. The results consider the precision (i.e., the uncertainty in the position estimates) and the accuracy (i.e., the difference between the real position of the nodes and the position determined by the localization algorithm) of the proposed approach. We compare the results with other well-known range-based localization approaches (DV-distance [9] and multilateration [10], [11]). The precision of our approach is also compared with the Cramer-Rao lower bound (CRLB).

A. Cramer-Rao Lower Bound

The CRLB is a lower bound which can be used to evaluate the variance of any unbiased estimator [24]. Assuming that there are M beacons and N unknowns in the network, let $\theta = [x_1, x_2, \dots, x_N, y_1, y_2, \dots, y_N]$ be the coordinate variables to be estimated. The likelihood function is:

$$f(\lg \mathbf{d}; \theta) = \prod_{j=1}^{M+N} \prod_{\substack{i \in H(j) \\ i < j}} e^{-\frac{(\lg d_{i,j} - \lg \bar{d}_{i,j})^2}{2\sigma_D^2}}, \quad (22)$$

where $i \in H(j)$ means node i is within j 's transmission range. The CRLB can be calculated based on $2N \times 2N$ Fisher Information matrix $I(\theta)$ [25]:

$$[I(\theta)]_{k,j} = \begin{cases} \sum_{i \in H(j)} \beta \frac{(x_i - x_j)^2}{\bar{d}_{i,j}^4} & k = j \\ \beta \frac{(x_k - x_j)^2}{\bar{d}_{i,j}^4} & k \neq j, k \in H(j) \\ 0 & \text{otherwise} \end{cases} \quad (23)$$

if $1 \leq k \leq N$ and $1 \leq j \leq N$,

$$[I(\theta)]_{k,j} = \begin{cases} \sum_{i \in H(j)} \beta \frac{(x_i - x_j)(y_i - y_j)}{\bar{d}_{i,j}^4} & k = j \\ \beta \frac{(x_k - x_j)(y_k - y_j)}{\bar{d}_{i,j}^4} & k \neq j, k \in H(j) \\ 0 & \text{otherwise} \end{cases} \quad (24)$$

if $1 \leq k \leq N$ and $N+1 \leq j \leq 2N$, or $1 \leq j \leq N$ and $N+1 \leq k \leq 2N$,

$$[I(\theta)]_{k,j} = \begin{cases} \sum_{i \in H(j)} \beta \frac{(y_i - y_j)^2}{\bar{d}_{i,j}^4} & k = j \\ \beta \frac{(y_k - y_j)^2}{\bar{d}_{i,j}^4} & k \neq j, k \in H(j) \\ 0 & \text{otherwise} \end{cases} \quad (25)$$

if $N+1 \leq k \leq 2N$ and $N+1 \leq j \leq 2N$. The constant β is inversely proportional to σ_D and $\bar{d}_{i,j}$ is the distance between node i and node j . Therefore, variance of each estimated parameter is lower bounded by $\sigma_{\theta_i}^2 \leq [I^{-1}(\theta)]_{i,i}$.

B. Performance Evaluation

For the simulation we considered 50 unknowns and 6 beacons randomly placed in a square area (of variable size depending on the desired density). The transmission radius was restricted to 13.5m (corresponding to an RSSI measurement of 78). We evaluated the effect of the variation of several parameters (number of hops the information is allowed to travel, density, number of unknowns, number of beacons and measurement inaccuracy), on the accuracy and the precision of the proposed approach. Unless otherwise specified, we used a node density of 0.03 nodes/ m^2 and a standard deviation for the RSS of 2.5 dB (corresponding to the value obtained from calibration measurements). For every graph we present the average of 20 simulations with different network topologies. All the results are normalized with respect to the transmission range.

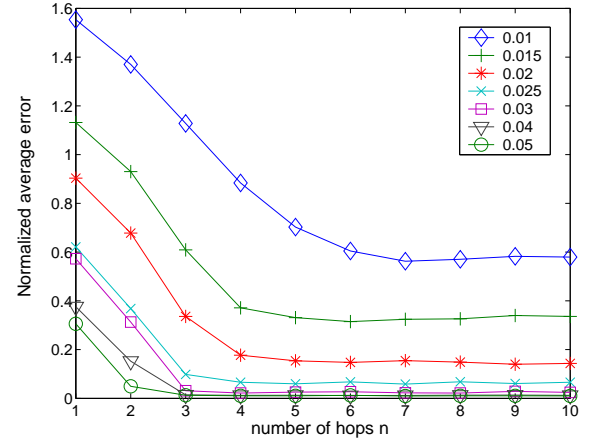


Fig. 8. Accuracy of the proposed approach as a function of the number of hops from the beacons to the unknown nodes for different node densities.

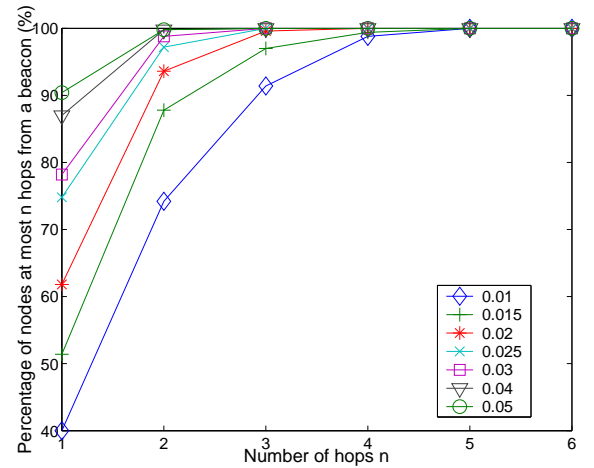


Fig. 9. The percentage of nodes reachable by at least one beacon in n hops as a function of n for different node densities.

1) *The Effect of the Number of Hops between Beacons and Unknowns:* To evaluate the number of hops after which

a beacon information becomes irrelevant we simulated the network and varied the number of hops that the beacon packets are allowed to travel from the beacon nodes. To eliminate the influence of measurement noise, we just ignored it in this simulation (but included it in all other simulations). The accuracy of the proposed approach as a function of the number of hops that beacon information is allowed to travel is shown in Fig. 8. Different lines correspond to different network densities.

For sparse networks, unknown nodes are unable to hear directly from the beacons, and, hence, have to rely on information propagated through multiple hops. Figure 8 shows that, regardless of the network density, it is clear that information does not have to travel far before the proposed approach converges: information from distant beacons cannot significantly improve the accuracy of the proposed approach. Thus, we can claim that in the proposed approach unknown nodes only need local (a few hops away) information to localize themselves.

Figure 9 shows the percentage of nodes that are within n hops range of at least one beacon for the same densities in Fig 8.

In what follows, all approaches are evaluated through two aspects: the accuracy (average estimation error) and the precision (standard deviation of the location estimate). For the proposed approach, results, both before and after the negative constraint refinement are shown in all the figures in order to highlight the influence of the negative constraints on the performance of the proposed system.

2) *The Effect of the Network Density:* In this simulation we studied the effect of the network density on the accuracy of the proposed approach. To change the density we changed the deployment area and kept the number of beacons and unknowns constant. The accuracy and the precision results are presented in Fig. 10 and Fig. 11 respectively.

Both the accuracy and the precision improve with the increase of the network density. This is not surprising as the CRLB is rather sensitive to the number of neighbors of a node. Similarly, in the proposed approach, the more neighbors, the more constraints will be placed on the unknowns. Another reason for the poor performance at lower densities is that (as shown in Fig. 9) the unknowns are relatively too far from the beacon nodes to obtain any estimation improvements. The negative constraints improve the effectiveness of the proposed approach considerably: the performance is very close to the optimum (the CRLB).

3) *The Effect of the Number of Unknown Nodes:* In this scenario we varied the number of unknowns from 10 to 100 (while maintaining the density constant). The average errors and the standard deviation of the estimation are shown in Fig. 12 and 13 respectively. The standard deviation for all methods increase as the number of unknowns increases, while the CRLB is almost constant. The intuition behind this result is that only the beacon nodes are aware of their positions and introduce information into the system: the unknown nodes will estimate their positions based on the information from the beacons. As the number of unknowns increases, the numbers

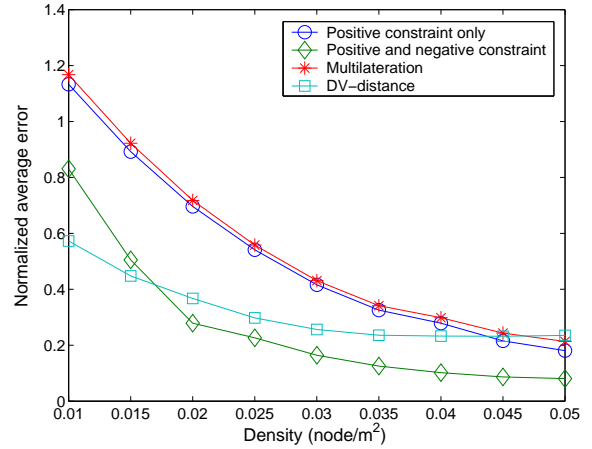


Fig. 10. The effect of network density on localization accuracy.

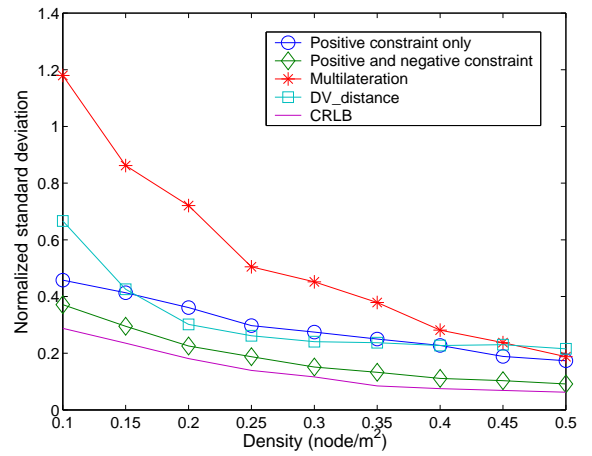


Fig. 11. The effect of network density on localization precision

of hops from beacons to most of the unknowns increase as well (recall that the node density is kept constant), thus the information from the beacons will be diluted by going through multiple hops. The constant number of neighbors and beacons account for the almost constant CRLB.

4) *The Effect of the Number of Beacon Nodes:* To evaluate the effect of the number of beacons on the proposed approach we varied their number from 3 to 10. The results are shown in Fig. 14 and Fig. 15. The CRLB indicates that the localization precision does not change significantly with the number of beacons. When the number of beacons increases the precision of all approaches increases.

5) *The Effect of the Range Measurement Inaccuracy:* Finally, we studied the effect of the inaccurate measurements on the accuracy and the precision of the proposed approach, by increasing the standard deviation of the RSS (σ_P). We varied σ_P between 0.5dB to 5dB (recall that the average σ_P from calibration measurements is approximately 2.5dB). The results are shown in Fig. 16 and Fig. 17. The CRLB increases proportionally to σ_P . The performance of all algorithms follows this increasing tendency, worsening their performance as the

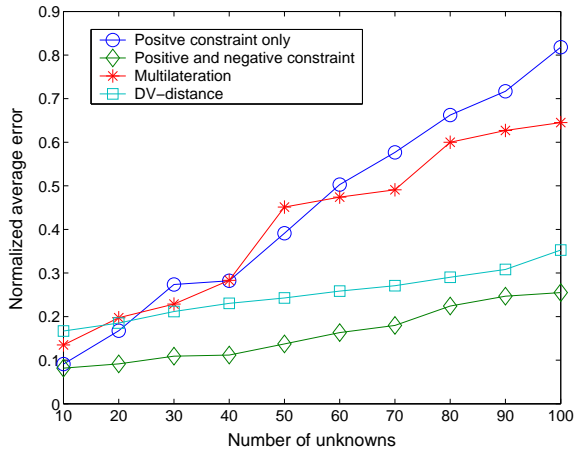


Fig. 12. The effect of the number of unknowns on localization accuracy.

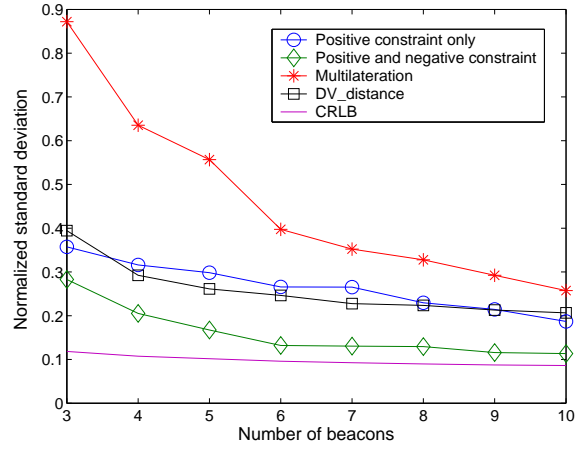


Fig. 15. The effect of the number of beacons on localization precision.

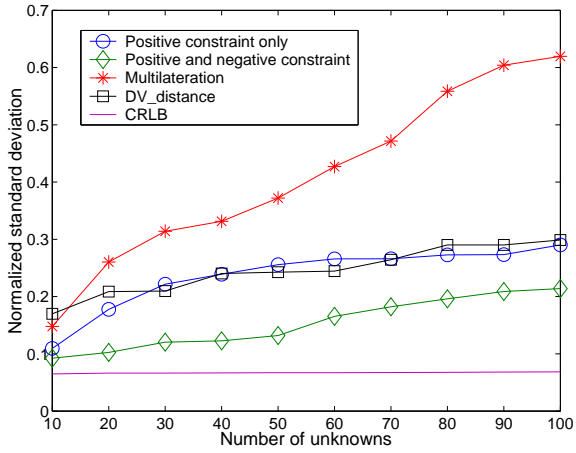


Fig. 13. The effect of the number of unknowns on localization precision.

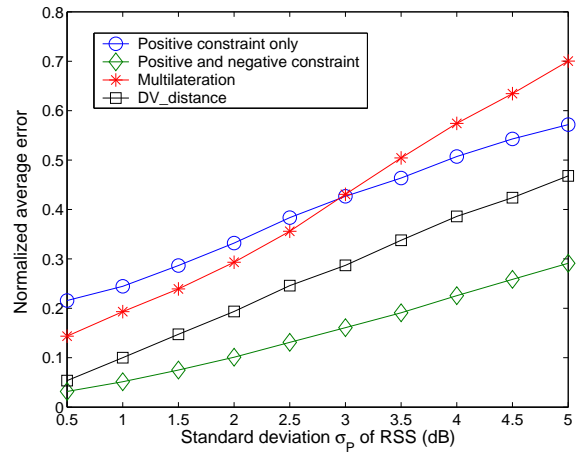


Fig. 16. The effect of range inaccuracy on localization accuracy.

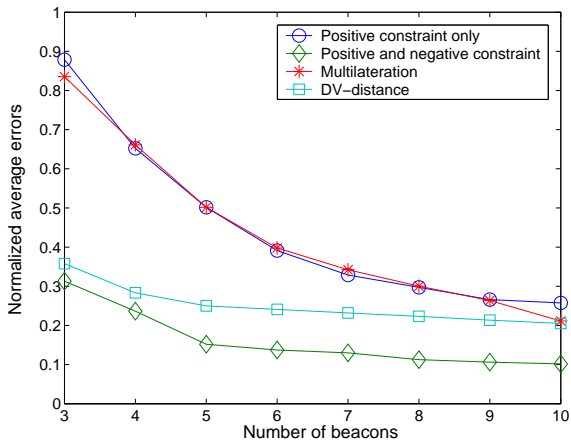


Fig. 14. The effect of the number of beacons on localization accuracy.

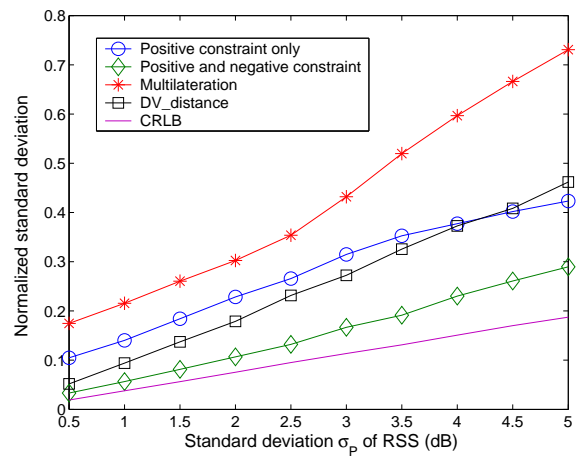


Fig. 17. The effect of range inaccuracy on localization precision.

measurements become more inaccurate.

All the performance results share some common characteristics:

- the negative constraints considerably improve the accuracy and the precision of the proposed approach;
- the proposed approach consistently outperforms other existing localization approaches;
- the precision of the proposed approach is, in many situations, very close to the theoretical optimum (the CRLB).

C. Implementation Issues

As suggested by Fig. 8, information from the beacons has to travel only a few hops for the approach to be effective. Thus, while the beacon packets become larger as they travel from the beacons (by two to three bytes per hop), the beacon packets do not have to be more than 15-20 bytes long.

While probabilistic approaches are relatively computationally expensive, a mica2 mote can compute and intersect two constraints in 15 seconds [5]. Thus, it can be expected that the entire localization approach will take a few minutes; for most applications expecting months to years of service from the sensor network this is a relatively small price to pay for accurate localization information.

The processing time can be further reduced if each node only computes constraints for the locations where its current position estimate is not zero - a very simple enhancement that can substantially reduce the computing time.

VI. CONCLUSION

In this paper, we presented a distributed, RSS-based localization approach for wireless sensor networks. The approach accounts for inaccurate range measurements by using probability functions for range measurements. Both positive and negative constraints originating at the beacons reduce the uncertainties of the positions of the unknown nodes. The approach is shown to outperform existing range-based localization approaches and perform close to the Cramer-Rao lower bound.

ACKNOWLEDGMENTS

We sincerely thank the anonymous reviewers for their constructive and detailed comments.

REFERENCES

- [1] I. Akyildiz, W. Su, Y. Sankarasubramaniam, and E. Cayirci, "A survey on sensor networks," *IEEE Communication Magazine*, vol. 40, no. 8, pp. 102–116, Aug. 2002.
- [2] —, "Wireless sensor networks: A survey," *IEEE Computer*, vol. 38, no. 4, pp. 393–422, Mar. 2002.
- [3] G. Asada, T. Dong, F. Lin, G. Pottie, W. Kaiser, and H. Marcy, "Wireless integrated network sensors: Low power systems on a chip," in *Proc. of the 24th European Solid-State Circuits Conference*, The Hague, Netherlands, 1998. [Online]. Available: citeseer.nj.nec.com/278712.html
- [4] V. Ramadurai and M. L. Sichitiu, "Localization in wireless sensor networks: A probabilistic approach," in *Proc. of the 2003 International Conference on Wireless Networks (ICWN 2003)*, Las Vegas, NV, June 2003, pp. 275–281.
- [5] M. L. Sichitiu and V. Ramadurai, "Localization of wireless sensor networks with a mobile beacon," in *Proc. of the First IEEE Conference on Mobile Ad-hoc and Sensor Systems (MASS 2004)*, Fort Lauderdale, FL, Oct. 2004.
- [6] P. Bahl and V. Padmanabhan, "RADAR: An in-building RF-based user location and tracking system," in *Proc. of Infocom'2000*, vol. 2, Tel Aviv, Israel, Mar. 2000, pp. 775–584.
- [7] N. Priyantha, A. Chakraborty, and H. Balakrishnan, "The cricket location-support system," in *Proc. of International Conference on Mobile Computing and Networking*, Boston, MA, Aug. 2000, pp. 32–43.
- [8] D. Niculescu and B. Nath, "Ad-hoc positioning system," in *Proc. of IEEE GLOBECOM*, 2001.
- [9] —, "DV Based Positioning in Ad hoc Networks," *Telecommunication Systems*, 2003.
- [10] A. Savvides, C. C. Han, and M. B. Srivastava, "Dynamic fine-grained localization in ad-hoc networks of sensors," in *Proc. of Mobicom'2001*, Rome, Italy, July 2001, pp. 166–179.
- [11] A. Savvides, H. Park, and M. Srivastava, "The bits and flops of the n-hop multilateration primitive for node localization problems," in *First ACM International Workshop on Wireless Sensor Networks and Applications*, Atlanta, GA, Sept. 2002.
- [12] C. Savarese, J. M. Rabaey, and J. Beutel, "Locationing in distributed ad-hoc wireless sensor networks," in *Proc. of ICASSP'01*, vol. 4, 2001, pp. 2037–2040.
- [13] S. Capkun, M. Hamdi, and J. P. Hubaux, "GPS-free positioning in mobile ad-hoc networks," *Cluster Computing*, vol. 5, no. 2, April 2002.
- [14] D. Moore, J. Leonard, D. Rus, and S. Teller, "Robust Distributed Network Localization with Noisy Range Measurements," in *Second ACM Conference on Embedded Networked Sensor Systems*, Nov. 2004, pp. 50–61.
- [15] X. Ji and H. Zha, "Sensor Positioning in Wireless Ad-hoc Sensor Networks Using Multidimensional Scaling," in *IEEE INFOCOM*, Mar. 2004, pp. 2652–2661.
- [16] D. Niculescu and B. Nath, "Ad hoc positioning system (APS) using AOA," in *IEEE INFOCOM*, Apr. 2003.
- [17] A. Nasipuri and K. Li, "A directionality based location discovery scheme for wireless sensor networks," in *First ACM International Workshop on Wireless Sensor Networks and Applications*, Atlanta, GA, Sept. 2002.
- [18] R. Want, A. Hopper, V. Falco, and J. Gibbons, "The active badge location system," *ACM Transactions on Information Systems*, vol. 10, pp. 91–102, Jan. 1992.
- [19] N. Bulusu, J. Heidemann, and D. Estrin, "GPS-less low cost outdoor localization for very small devices," *IEEE Personal Communications Magazine*, vol. 7, pp. 28–34, Oct. 2000.
- [20] L. Doherty, K. S. J. Pister, and L. E. Ghaoui, "Convex position estimation in wireless sensor networks," in *Proc. IEEE Infocom 2001*, vol. 3, Anchorage AK, Apr. 2001, pp. 1655–1663.
- [21] A. Galstyan, B. Krishnamachari, K. Lerman, and S. Patten, "Distributed Online Localization in Sensor Networks Using a Moving Target," in *the third international symposium on information processing in sensor networks*, 2004, pp. 61–70.
- [22] T. He, C. Huang, B. M. Blum, J. A. Stankovic, and T. Abdelzaher, "Range-Free Localization Schemes for Large Scale Sensor Networks," in *ACM MobiCom*, 2003, pp. 81–95.
- [23] T. S. Rappaport, *Wireless Communications: Principles and Practice*, 2nd ed. Pearson Education, 2001.
- [24] S. M. Kay, *Fundamentals of Statistical Signal Processing, Volume I: Estimation Theory*, 1st ed. Prentice Hall, 1993.
- [25] N. Patwai, A. O. Hero, M. Perkins, N. S. Correal, and R. J. O'dea, "Relative Localization Estimation in Wireless Sensor Network," *IEEE Transactions on Signal Processing*, vol. 51, pp. 2137–2148, Aug. 2003.